Ihor Karkhut

STRENGTH OF INCLINED CROSS-SECTIONS OF REINFORCED CONCRETE PROTECTIVE SHELLS UNDER THE ACTION OF PUNCHING

Lviv Polytechnic National University,
Department of Building Constructions and Bridges
karkhoot1@gmail.com

The experience of inclined cross-sections in the zones of influence of transverse forces and punching loads has been studied. The results of experimental studies of inclined cross-sections of protective structures in the area of influence of local emergency load on punching are presented. The article presents the reinforcement and strength of inclined cross-sections at the angle of destruction $\gamma = 40°$. The analysis of the results was carried out and recommendations were developed for the design of inclined cross-sections of shells in the punching zone. The experimentally obtained values of the bearing capacity of concrete and reinforced concrete samples during punching correlate well with the results of theoretically determined dependencies that take into account the pin effect of reinforcement and the actual strength of concrete.

Key words: protective structure; aircraft crash; heavy concrete; punching; horizontal reinforcement; inclined sections.
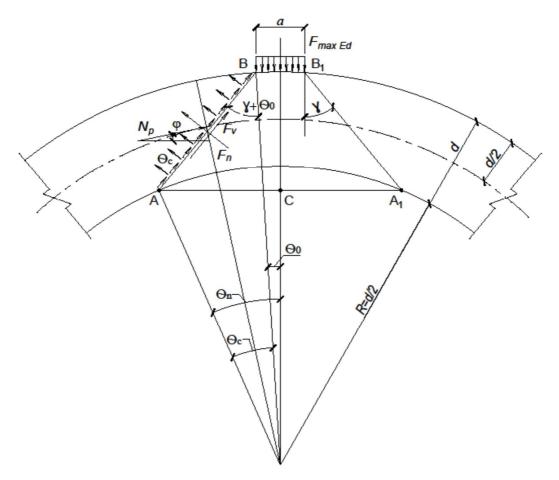
Introduction

The purpose of this work was to investigate the strength of reinforced concrete slabs and shells in the zone of punching by an emergency dynamic load, to develop proposals for taking into account the effect of horizontal reinforcement on the strength of inclined cross-sections. As a result of the analysis of the results of experimental studies of fragments of thin shells, to propose recommendations for the design of inclined cross-sections of monolithic reinforced concrete shells of protective structures with additional horizontal reinforcement in the punching zone under emergency loading.

The protective shells of energy and other facilities have different design schemes, which can be classified according to the shape, lining material and biological protection, deepening into the soil. All of them are united by the fact that they have reinforced concrete walls (Karkhut, 2015; Eibl, 2003; Raghupati, 1999; Briffaut, 2011) for various purposes and an annular section. In emergency conditions, these thin reinforced concrete shells are affected by increased internal pressure and elevated temperature up to 150 °C from the coolant. The regime of a major accident that occurred at the Chernobyl NPP during the destruction of the reactor core can lead to the destruction of the containment by internal pressure due to the insufficient bearing capacity of this structure. The emergency modes of thermal force loads also include the action of local influences, such as the impact of a crashed aircraft. The impact of such a large mass causes a local increase in the temperature of the outer surface and shear stresses in the containment concrete, which can cause destruction along inclined cross-sections (Eibl, 2003; Králik, 2014; Makarenko, 1986; Duan, 2018; Luchko, 2018; Sadique, 2013; Lo Frano, 2011). The main provisions of the calculation hypotheses of the strength of inclined cross-sections of the containment shell to the action of such an emergency local load from an aircraft crash (Makarenko, 1986; Duan, 2018; Luchko, 2018; Lo Frano, 2011) are that this load acts perpendicular to the shell surface (Fig. 1), and its application rate is taken according to the IAEA recommendations. The contact surface area of this load from the fall of the Fantom-

4F aircraft with the shell is 7–14 m². The mathematical model of the load is taken in the form of elastic-viscous or elastic-viscoplastic systems, the reaction of which, when interacting with the protective reinforced concrete shell, determines the dynamic emergency load (Eibl, 2003; Makarenko,1986; Luchko, 2018; Lo Frano, 2011).

The problem of determining the design load is solved by solving the system of equations of shell motion under the action of this load and a piecewise linear integral equation of the first kind using d'Alembert's initial conditions. The corresponding force component of the emergency load (Eibl, 2003; Makarenko, 1986) is calculated by the Laplace integral transform method, taking into account the ratio of the containment stiffness and aircraft structure.

Fig. 1. The scheme of the destruction of the containment
during the fall of the aircraft

The local load on the circular area of contact with the shell, the diameter of which *a* is equal to the diameter of the aircraft fuselage, is determined from the equation (1):

$$P(t) = 4F(t)/\pi a.^2 \tag{1}$$

The change in the function $F(t)$ in time has the form of a periodic curve, exponentially decaying, asymptotically approaching zero. Taking into account the sharp decrease in the amplitude of the load function after the first half-cycle of oscillations, practical calculations are limited to this time. This load can cause local failure along the side surface in the form of a sheared cone.

In this case, the hypothesis (Makarenko, 1986) is considered valid, according to which the limit state on the fracture area occurs simultaneously from tensile and shear stresses uniformly distributed over the cross-sectional area. The angle of destruction γ in this case depends on the rate of application of the load

and the initial stress state. It was assumed that the normal and tangential stresses are uniformly distributed, since the cross-sections operate under conditions of limited deformations, and depend on the dynamic tensile strength of concrete. The condition of strength in the limit state for a reinforced concrete shell without prestressing in the zone of influence of the punching load is written by equation (2):

$$F_v \cdot cos\ \gamma + F_n \cdot sin\ \gamma = F_{maxRd}, \tag{2}$$

where F_v and F_n are the integral values of the tangential and normal components of the stress vector, $F_{max\ Ed}$ is the vector of the external load module. It was recommended to determine the tangential and normal components of the stress vector according to the following dependencies:

$$F_v = 2k_dR_{bt}A, \tag{3}$$

and

$$F_n = k_dk_wR_{bt}A. \tag{4}$$

The coefficient of dynamic strengthening of concrete kd in these dependencies is recommended to be calculated according to the proposals (Karkhut, 2015; Makarenko, 1986) and taken within 1.0–1.3 depending on the speed of application of the external load and the level of concrete prestressing. The calculated area A was determined according to the design scheme of punching (Fig. 1) from the condition:

$$A = \pi AB \cdot (a + AB \cdot sin\ \gamma). \tag{5}$$

For the load application rate $v = 2.5 \cdot 10^4$ kN/(m²c), which corresponds to the fall of the aircraft body, the angle $\gamma \approx 40°$. The coefficient of transverse reinforcement in the form of clamps kw was taken equal to 1.4 in their presence and 1.0 in their absence.

The presented scheme of dynamic punching load differs from the scheme for static loads (Babaev, 2015; Blikharskyy, 2017). In the boundary state, the concept of control perimeters is used, the first of which is located at a distance of $2d$ (d is the working height of the cross-section) from the zero perimeter or the boundary of the external load application. In this case, the angle of destruction $\gamma = 63.4°$. It is recommended (Babaev, 2015) to include in the calculation a bend outside the area of the external load, if the distance from it to the edge of the load is ≤0.25d.

The operation of the transverse reinforcement of the stirrups, normal to the longitudinal axis of the thin plate or shell, is complicated in terms of its anchoring:

– welding of stirrups to the nodes of the upper and lower horizontal reinforcing meshes or sheets often does not provide anchoring due to insufficient adhesion of reinforcement to concrete, or short length of stirrups, especially in thin slabs and shells;

– the installation of stirrups as part of additional frames, manufactured at the factory using contact welding, leads to the appearance of additional longitudinal bars at the level of the lower and especially the upper reinforcing mesh, which makes concreting difficult, it is possible to "burn" the rods;

– installation of stirrups in the form of studs or individual bars with special washers at the ends is technologically complex;

When arranging bends of horizontal reinforcement of meshes from the upper zone of the slab above the support to the lower zone or inclined clamps within the punching prism, the following problems arise:

– the place of application of the emergency load is unknown and, accordingly, the place and other geometric parameters for making bends or stirrups are unknown;

– bends and stirrups become very indefinite due to the need to take into account the design bending radii of the bars (with indefinite cross-section angles with the punching prism surface), which is especially felt for plates and shells with a thickness of less than 300–400 mm. Also known are the results of studies under the action of transverse forces on the punching of beams, plates and shells with the use of horizontal bars (Maksymovych, 2019; Maksymovych, 2020), showing the possibility and efficiency of using such reinforcement. These papers present the results of studies conducted at the Lviv Polytechnic and NDIBK (Kyiv) (Babaev, 2015; Blikharskyy, 2017).

The impact of the pin effect and the stress diagrams along the length of the horizontal bars are shown in Fig. 2. When developing the design hypothesis, it was assumed that the plastic properties of concrete are sufficient for the bearing capacity of the punching zone (similar to the methodology of the current standards) to be determined by the sum of the bearing capacity of concrete and reinforcement:

$$V \leq V_c + V_{sw},$$ (6)

where V_c was taken equal to the right side of inequality (Babaev, 2015):

$$F \leq \alpha R_{bt} u_m d.$$ (7)

In this inequality, um is half the sum of the lengths of the zero and first control perimeters, and the coefficient $\alpha = 1.0$ for heavy concrete.
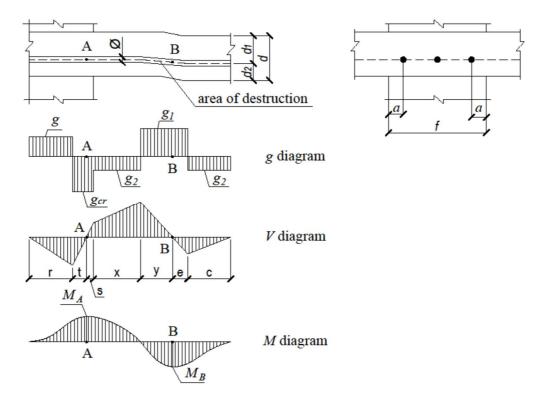

Fig. 2. The work of horizontal reinforcement on a transverse force

When assessing V_{sw}, it was assumed that the plastic properties of the materials are sufficient to realize close-to-rectangular concrete pressure diagrams on the reinforcing bar, and the bending moment M_{max} was determined by the plastic modulus of resistance W_{pl} and the calculated reinforcement resistance f_{yd} for a given bar Ø. Then:

$$W_{pl} = 0.166 \, Ø.^3$$ (8)

$$M_{max} = 0.166 \, Ø^3 f_{yd}$$ (9)

and the bearing capacity V_{sw} of a horizontal reinforcing bar during its work on the transverse shear of concrete was determined as the minimum at which the maximum possible pressure on concrete g_1, g_2, gcr and maximum bending moments at least at one of points A and B (Fig. 2) are achieved.

Taking into account the known dependencies between the diagrams g, V i M, an equilibrium equation was obtained at points A and B. For equilibrium conditions around point B, the maximum value V^B_{max} is calculated from the condition:

$$V_{max}^{B} = 0.576 \cdot \sqrt{f_{yd} g_1 Ø^3}$$ (10)

Similarly, for equilibrium conditions around point A, the maximum value V^A_{max} at $x = 0$ is calculated by the condition:

$$V^A_{max} = 0.576 \cdot \sqrt{f_{yd} g_{cr} \varnothing^3} \tag{11}$$

And the smallest value V^A_{max} – if $S = 0$ (location of point A on the edge of the load application) is calculated from the condition:

$$V^A_{max} = 0.576 \cdot \sqrt{f_{yd} g_2 \varnothing^3} \tag{12}$$

and

$$x = 0.576 \cdot \sqrt{\frac{(f_{yd} \varnothing^3)}{g_2}} \tag{13}$$

The change in the value of V_{max} depending on the x coordinate (Fig. 4) was analyzed and it was recommended for practical calculations to determine V_{max} according to (11).

Based on the obvious expediency of the condition $V^A_{max} = V^B_{max}$, $g_1 = g_2$ should be ensured, therefore $d_1 = d_2$, that is, additional reinforcement was recommended to be placed in the middle of the cross-section height. It was proposed to determine the minimum required length of the bar beyond the limit of the punching force to ensure anchoring from the condition:

$$L = 1.96 \cdot \sqrt{\frac{(f_{yd} \varnothing^3)}{g_1}} \tag{14}$$

Consequently, the problem was considered solved for known values of $g_1 = g_2$. Regarding g, the following assumptions were made:

    – g_1 cannot be greater than the local compressive strength of concrete:

$$g_{11} \leq R_{b,loc} \varnothing \tag{15}$$

where $R_{b,loc}$ – in accordance with (Babaev, 2015);

    – g_1 cannot be greater than:

$$g_{12} \leq R_{bt} (d - \varnothing), \tag{16}$$

where R_{bt} – in accordance with (Babaev, 2015);

    – g_1 cannot be greater than:

$$g_{13} \leq R_{bt} \cdot (f - 2a + d - \varnothing)/m. \tag{17}$$

In inequality (17), all designations in accordance with Fig. 2, where f is the width of the load application band (corresponds to the dimension a in Fig. 1); a is the distance from the loading edge to the horizontal reinforcement rod within the loading area ($a \leq s/2$ can be taken as a margin of safety, which corresponds to half the horizontal reinforcement pitch); m is the total number of bars that cross the line of action of the punching load (control perimeter) and perceive part of the punching force.

Then the bearing capacity of the horizontal reinforcement for the punching action is calculated from the dependence:

$$F^h_{sw} = 0.576 \cdot m \cdot \sqrt{f_{yd} g \varnothing^3} \tag{18}$$

Where g is the smaller of the three values determined by (15), (16), (17). To reinforce inclined sections, various structural measures and materials are used, including steel bars and fibers, non-metallic fibers, carbon tapes and sheets (Blikharskyy, Khmil, 2017; Bobalo, 2018; Selejdak, 2020; Cavagnis, 2020; Maksymovych, 2019). Such methods are effective when there is access to inclined cross-sections of bending elements along the height, and when there is access only to the upper and lower faces, they are

used to strengthen normal sections. In the study of the strength of bending elements without transverse reinforcement (Maksymovych, 2019), the appearance and development of critical inclined cracks were described, the development of which at fracture angles less than 45° has not been studied.

Based on the results of the review of the state of studying the strength of inclined cross-sections, the following conclusions can be drawn:

–   there are several methods for calculating the design and reinforcement of cross sections that can be used to assess the strength under dynamic emergency loading;

–   the accuracy of many approaches and solutions for determining the bearing capacity and reinforcing of inclined cross-sections under emergency actions remains uncertain;

–   in thin slabs and shells, the installation of additional horizontal reinforcement leads to an increase in the bearing capacity for punching;

–   when designing, the same values of g_{12} according to (16) and g_{13} according to (17) should be ensured, and the value of g_{11} according to (15) is almost never decisive;

–   the influence of horizontal reinforcement on the strength of inclined cross-sections under dynamic impacts is unknown, therefore it is recommended to limit the cases to $F_{max}/F_c \leq 1.6$;

–   anchoring length of horizontal reinforcement L is always provided and can be taken as $L \geq 20\emptyset$.

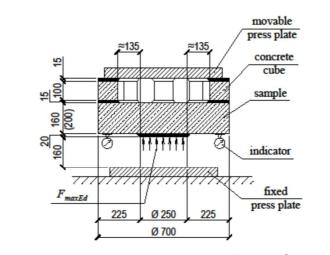Considering the above, the following tasks were solved in this work:

–   to develop a methodology for experimental studies of the strength of inclined cross-sections of protective structures for punching through a local emergency load;

–   to conduct experimental studies of samples – fragments of a monolithic shell of a protective structure with horizontal reinforcement;

–   develop proposals for the calculation and design of inclined cross-sections of the shell using horizontal reinforcement.

Materials and Methods

The strength of inclined cross-sections under the action of an emergency punching load was studied on reinforced concrete and concrete models of protective shells. The punching force (Fig. 3, 4) was applied perpendicular to the sample surface on a round area, which corresponded to the calculated static model of the emergency dynamic load (Fig. 1). Concrete cubes installed along the perimeter of the sample modeled a support distributed along the perimeter of the circle at a distance of ≈135 mm from the load application boundary. The destruction angle was close to 40° at the assumed sample thickness d, which was 160 mm. A partial effect of compression was achieved with reinforcement Ø12 class A240 at the ends of the working bars of the meshes in the form of a ring. This reinforcement also provided anchoring of the working mesh bars. The load was applied in stages with a holding time of 7–15 minutes to monitor the state of the samples, record the readings of measuring instruments, and measure the width of the cracks. At the actual load application speed, the dynamic coefficient $k_d = 1.0$. All materials for the manufacture of samples met the requirements of current standards (Concrete and reinforced concrete structures made of heavy concrete. Design rules. DSTU, 2011; Karkhut, 2021). Production and care of concrete was carried out in accordance with the requirements of current standards in the factory. Working reinforcement class A400C with $f_{yd} = 364$ MPa of a periodic profile Æl2 (3 samples), Æl6 (6 samples) was used (Table 1) in the form of flat welded meshes (Fig. 5). Ensile strength of concrete f_{ctm} was determined by splitting standard cubes. The geometric characteristics and properties of concrete and reinforcement of the samples are also given there.
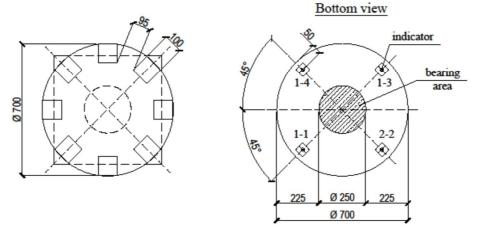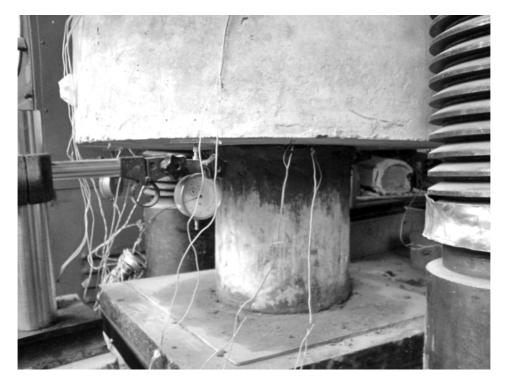
Fig. 3. Test model and instrument layout

Fig. 4. Sample prepared for testing

Table 1

Characteristics of concrete and reinforcement of samples

Sample designa-tion	f_{cd}, MPa	Tensile strength of concrete, MPa				Diameter of reinforcement Ø, mm	Number of bars, m for (17)	A_{sh}, cm²
		R_{bt} norm	$f_{ctk,0.05}$, norm	f_{ctm}, exper.	f_{ctm}, norm			
3-1	7.5	0.66	0.80	0.17	1.20	16	8	16.08
3-2	11.5	0.90	1.30	0.36	1.90	12	12	13.57
3-3	7.5	0.66	0.80	0.17	1.20	16	8	16.08
3-4	11.5	0.90	1.30	0.36	1.90	16	12	24.12
3-5	11.5	0.90	1.30	0.36	1.90	–	–	–
3-6	7.5	0.66	0.80	0.17	1.20	–	–	–
3-7	11.5	0.90	1.30	0.36	1.90	16	12	24.12
3-8	7.5	0.66	0.80	0.17	1.20	–	–	–
3-9	7.5	0.66	0.80	0.17	1.20	12	8	9.05
3-10	11.5	0.90	1.30	0.36	1.90	16	8	16.08
3-11	7.5	0.66	0.80	0.17	1.20	16	8	16.08
3-12	7.5	0.66	0.80	0.17	1.20	12	12	13.57

The physical and mechanical characteristics of concrete in compression were determined by testing standard cubes and prisms. A total of 12 round reinforced concrete and concrete fragments Ø700 mm were tested. The mesh in the reinforced samples was placed in the middle of the height of the sample. Samples 3-5, 3-6, 3-8 were tested without additional horizontal reinforcement. In the calculation for punching (Table 1), reinforcing bars with an area A_{sh}, were taken, located at a distance of no more than 0.25d from the zero perimeter, according to the proposals (Babaev, 2015; Blikharskyy, 2017).

To control the deformations of the samples during testing, 4 dial indicators with a division value of 0.01 mm were installed, located along two mutually perpendicular diameters at a distance of 50 mm from the edge of the sample. The deformations of concrete on the tensioned face were measured by strain gauges based on 50 mm, and the crack opening width on the side and top faces was measured with an MPB-3 microscope.

Results and discussion

As a result of the tests, the breaking load was determined. Concrete samples were destroyed when normal cracks were formed due to the action of a bending moment (force F^n_{crc}). In the reinforced samples, at subsequent stages, through-shaped spatial cracks appeared (force F^v_{crc}), which caused the destruction of inclined sections from normal and tangential stresses (Fig. 6).

The destruction forces were compared with the calculated ones according to (3) and are given in Table 2. The distances given in the table to the upper face d_1 from the axis of the lower meshes and d_2 from the axis of the upper meshes of the samples were measured after destruction. In some samples, vertical cracks formed on the side surface during destruction, and in some also horizontal cracks in the middle of the height (force F^h_{crc}), which indicated the destruction of concrete by splitting in the plane of the reinforcing mesh (Fig. 7).

Such destruction was recorded in samples with concrete class C10/12 and with insufficient adhesion of reinforcement to concrete. From the deflection diagrams (Fig. 8) of the samples, it can be concluded that an increase in the number of reinforcing bars of horizontal meshes along the width of the punching zone increases the bearing capacity. Thus, the strength of samples reinforced with three Ø12 bars in one direction with a pitch of 130 mm was higher than samples reinforced with a mesh of two Ø16 bars in one direction with a pitch of 250 mm, although the reinforcement area of 2Ø16 is larger than the area of 3Ø12.

Fig. 5. Reinforcement of samples

When calculating F_v and F_n (Table 2), the calculated area A according to (5) was taken equal to 0.253 m². The deviation of the experimental and theoretical values of the strength of inclined sections is significant. When taking into account the reinforcement, the deviation is 2–5 times, without taking into account the reinforcement for concrete samples, the deviation reaches 6 times.

This may be due to the fact that dependence (4) was derived for the case of using vertical stirrups and for the tensile strength of concrete R_{bt}, which is much higher than the experimentally obtained tensile strength of concrete during splitting.

Ihor Karkhut

a   b

Fig. 6. Destructive cracks on the upper: a – and lower; b – faces, sample 3-10

Fig. 7. Destruction of the side face of reinforced samples

Table 2

Experimental and calculated breaking forces (R_{bt} according norm)

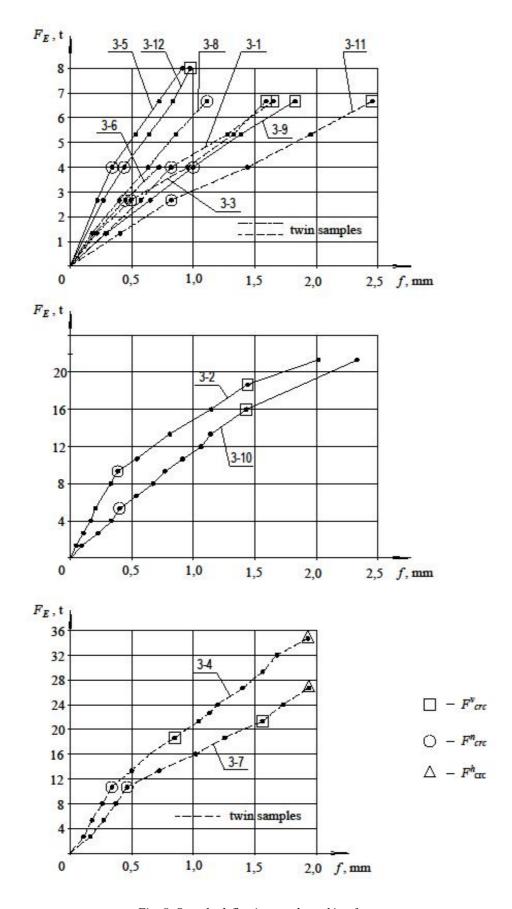| Sample designation	F_{maxEd}, kN	d_1, mm	$F_v \cos \gamma$ per (3), kN	$F_n \sin \gamma$ per (4), kN		F_{maxRd} per (2), kN	F_{maxEd} / F_{maxRd}	
				$k_w = 1$	$k_w = 1.4$		$k_w = 1$	$k_w = 1.4$
3-1	104.67	80	179.07	108.62	150.26	329.33	0.364	0.318
3-2	222.29	80	348.84	146.36	204.91	553.75	0.449	0.401
3-3	104.67	80	179.07	108.62	150.26	329.33	0.364	0.318
3-4	346.59	80	348.84	146.36	204.91	553.75	0.700	0.626
3-5	91.53	–	348.84	146.36	–	495.20	0.185	–
3-6	45.81	–	179.07	108.62	–	287.69	0.159	–
3-7	281.15	68	348.84	146.36	204.91	553.75	0.568	0.508
3-8	44.15	–	179.07	108.62	–	287.69	0.153	–
3-9	71.91	66	179.07	108.62	150.26	329.33	0.250	0.218
3-10	156.96	65	348.84	146.36	204.91	553.75	0.317	0.283
3-11	71.91	60	179.07	108.62	150.26	329.33	0.250	0.218
3-12	91.53	70	179.07	108.62	150.26	329.33	0.318	0.278

Fig. 8. Sample deflections and cracking forces

Table 3 shows the experimental and calculated values of the bearing capacity during punching according to various hypotheses. The force F_c (Table 3) was determined from dependence (7) (Babaev, 2015) taking into account the coefficient $160/135 = 1.185$ for a breaking angle of less than 45°. Since the use of the R_{bt} value according to (Babaev, 2015) leads to a significant overestimation of the actual punching strength, which is especially noticeable for concrete samples, the calculations were made with the replacement of R_{bt} by the experimentally determined values of f_{ctm}. With such a replacement, the deviation of the experimental data from the calculated ones is significantly reduced, but for many samples it is still more than 250–350 %.

Table 3

Strength of inclined cross-sections according to different hypotheses (experimental f_{ctm})

Sample designation	F_{maxEd}, kN	$F_v \cos\gamma$, kN	$F_n \sin\gamma$, kN	F_{maxRd}, kN per (2)	g, per (16, 17)		F^h_{sw}, kN per (18)	F_c, kN per (7)	$F^h_{sw} + F_c$ kN
					g_{12}, kN/m	g_{13}, kN/m			
3-1	104.67	65.72	38.72	104.50	24.48	8.373	16.30	37.96	54.26
3-2	222.29	139.17	82.12	221.29	53.28	11.94	18.97	80.41	99.38
3-3	104.67	65.72	38.72	104.50	24.48	8.373	16.30	37.96	54.26
3-4	346.59	139.17	82.12	221.29	51.84	11.82	29.06	80.41	109.47
3-5	91.53	139.17	58.66	197.83	–	–	–	80.41	80.41
3-6	45.81	65.72	27.70	93.42	–	–	–	37.96	37.96
3-7	281.15	139.17	82.12	221.29	51.84	11.82	29.06	80.41	109.47
3-8	44.15	65.72	27.70	93.42	–	–	–	37.96	37.96
3-9	71.91	65.72	38.72	104.50	25.16	8.458	10.64	37.96	48.60
3-10	156.96	139.17	82.12	221.29	51.84	17.73	23.72	80.41	104.13
3-11	71.91	65.72	38.72	104.50	24.48	8.373	16.30	37.96	54.26
3-12	91.53	65.72	38.72	104.50	25.16	5.638	13.03	37.96	50.99

Such significant deviations when compared with the method (Makarenko, 1986) can be explained by the fact that this method was developed to take into account vertical stirrups working in tension, but in fact it is necessary to take into account the pin effect that occurs when using horizontal reinforcement. The greatest error is introduced by the use of an integral reinforcement coefficient of 1.4. This can be seen from a significant decrease in the deviation for unreinforced samples, which is in the range of 13.8–20.7 %.

In the case of using horizontal grids, it would be logical to take into account the influence of such reinforcement on the increase in the force F_v due to the pin effect. Therefore, Table 4 shows the results of comparing the experimental bearing capacity with the calculated bearing capacity, which took into account Fv, obtained from dependence (3) according to the hypothesis (Eibl, 2003; Makarenko, 1986), taking into account the pin effect of horizontal reinforcement. In addition, the tensile strength of concrete obtained from the test of cubes for splitting was used. These results are in good agreement with the actual nature of the destruction. Thus, samples 3-1–3-4, 3-7, 3-10 failed simultaneously during bending and the formation of punching cracks and horizontal splitting cracks in the plane of the meshes, and concrete samples and reinforced 3-11, 3-12 collapsed in bending moment. The downward deviations of the calculated and experimental data are associated with the deviation of the horizontal meshes from the design position. All concrete specimens failed in bending, as the actual punching strength for them is twice as high. The same can be said for samples 3-1, 3-9, 3-10, which failed in bending due to the displacement of the meshes from the design position, and for specimens 3-11 and 3-12, which failed in bending. In these samples, at the stage of destruction, the first cracks from punching were formed (deviations in the downward direction in the range of 16–31 %). When ensuring the exact design position of the meshes, the deviation of the experimental values of the breaking load from the calculated ones did not exceed 5 %.

Table 4

Forces of crack formation and destruction during punching

Sample designation	F_{maxEd}, kN	$F_v \cos \gamma$, kN	$F_n \sin \gamma$, kN	F^h_{sw}, kN	F_{maxRd}, kN	F_{maxEd} / F_{maxRd}	The nature of the destruction
3-1	104.67	65.72	27.65	16.30	109.67	0.954	*M* and *F*
3-2	222.29	139.17	58.55	18.97	216.69	1.026	*M* and *F*
3-3	104.67	65.72	27.65	16.30	109.67	0.954	*M* and *F*
3-4	346.59	139.17	58.55	29.06	226.78	1.528	*M*, *F* and splitting
3-5	91.53	139.17	58.55	–	197.72	0.463	*M*
3-6	45.81	65.72	27.65	–	93.37	0.491	*M*
3-7	281.15	139.17	58.55	29.06	226.78	1.24	*M*, *F* and splitting
3-8	44.15	65.72	27.65	–	93.37	0.491	*M*
3-9	71.91	65.72	27.65	10.64	104.01	0.691	*M*
3-10	156.96	139.17	58.55	23.72	221.44	0.709	*M* and *F*
3-11	71.91	65.72	27.65	16.30	109.67	0.656	*M*
3-12	91.53	65.72	27.65	13.03	106.40	0.86	*M*

For concrete samples without reinforcement, the experimental and theoretical breaking moments in bending were compared. The points of transfer of the external force to the edge of the samples (Fig. 9) were taken at the center of gravity of the triangular pressure diagram, as for the supports of the bending elements, taking into account the deformable model. The experimental breaking moments were calculated relative to the points of application of the resultant external punching force for the cases of rectangular and triangular (Table 5) pressure diagrams, according to the possible nature of the deformation of the samples (Fig. 6), and the theoretical calculated breaking moments were calculated using dependence (23) (Karkhut, 2015; Babaev, 2015): $M_{Rd} = R_{bt}W_{pl}$, where the plastic moment of resistance of a rectangular section is $W_{pl} = bd\,2/3.5$. In this case, for comparison, the values of concrete tensile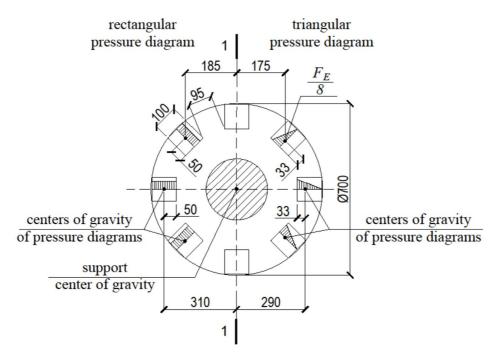 strength in bending R_{bt} according to (Babaev, 2015) and $f_{ctk,0.05}$ according to (Blikharskyy, 2017) were taken into account.

Fig. 9. To the calculation of concrete samples in bending

Table 5

Bending moments of destruction of concrete samples

Sample designation	W_{pl}, cm³	$F/8$, kN	Destructive moments, kNm				M_{exp}/M_{Rd} theoretical			
			M_{ekcn} at diagram		M_{Rd} theor. with R_{bt}	M_{Rd} theor. with $f_{ctk,0.05}$	M_{Rd} with R_{bt}		M_{Rd} with $f_{ctk,0.05}$	
			rectan-gular	triang-ular			rectan-gular	triang-ular	rectan-gular	triang-ular
3-5	4843	11.442	7.78	7.322	4.359	6.296	1.785	1.682	1.236	1.163
3-6	4843	5.721	3.89	3.661	3.196	3.875	1.217	1.145	1.004	0.945
3-8	4843	5.45	3.71	3.488	3.196	3.875	1.161	1.091	0.957	0.900

As can be seen from Table 5, the use of $f_{ctk,0.05}$ in calculations gives smaller deviations from the experimental data, they are in the range of 1.0–23.6 % for a rectangular pressure diagram and 5.5–16.3 % for a triangular one. When using the R_{bt} value, the maximum deviations increase to 78.5 % for a rectangular pressure plot and 68.2 % for a triangular one. For reinforced samples, the use of a triangular diagram that takes into account the deformation of the samples (deflection and rotation of the reference section) also gives a better agreement between the calculated and experimental values (Table 6). With a triangular pressure diagram, the maximum deviations are less by 12–13 % than with a rectangular one. From a comparison of the bearing capacity for punching samples without reinforcement with samples with additional horizontal reinforcement, it can be seen that the presence of horizontal reinforcement significantly increases the strength and reduces the deflection of the samples.

In general, the test results indicate that by the time of failure, the entire height of the concrete section works for punching, and the hypotheses (Eibl, 2003; Makarenko,1986; Blikharskyy, 2017) are valid, and not only the working height of the section d, as is customary in (Babaev, 2015; Blikharskyy, 2017) for static (punching angle more than 45°) and emergency dynamic loads with punching angles less than 45°. From the graphs in Fig. 8 it can be seen that the deformation and strength of the samples with the same reinforcement is significantly affected by the class of concrete. The strength is twice as low in samples of concrete of class C10/12 compared to concrete of class C16/20. In addition, in samples of C16/20 concrete, no fracture from splitting in the mesh plane was recorded, which makes it possible to recommend this class of concrete as the minimum for protective structures under the action of punching.

Table 6

Bending moments of destruction of reinforced concrete samples

Sample designation	A_s, mm²	$F/8$, kN	d, mm	Moments of destruction, kNm			M_{exp}/M_{Rd}	
				M_{exp} at diagram		M_{Rd} theor. per [13]	rectangular diagram	triangular diagram
				rectangular	triangular			
3-1	402	13.077	80	8.89	8.37	9.57	0.91	0.87
3-2	339	27.788	80	18.9	17.78	8.88	2.13	2.00
3-3	402	13.077	80	8.89	8.37	9.57	0.91	0.87
3-4	603	43.317	80	29.46	27.72	14.43	2.04	1.92
3-7	603	35.144	68	23.9	22.49	11.78	2.03	1.91
3-9	226	8.99	66	6.11	5.75	4.74	1.29	1.21
3-10	402	19.615	65	13.34	12.55	8.12	1.64	1.55
3-11	402	8.99	60	6.11	5.75	6.63	0.92	0.87
3-12	339	11.442	70	7.78	7.32	7.27	1.07	1.01

The results of experimental studies confirmed the possibility of determining the bearing capacity of reinforced concrete shells of protective structures with horizontal reinforcement under the action of an emergency local punching load according to the modified dependences of the hypothesis (Eibl, 2003; Makarenko,1986). When replacing the integral reinforcement factor in them when calculating F_n by an

additional force from the pin effect of reinforcement when calculating F_v the error does not exceed 13.8-20.7 %. In this case, the best agreement between the experimental and calculated values is obtained by using the f_{ctm} value obtained experimentally when splitting with bars, the diameter of which corresponds to the diameter of the reinforcement of horizontal meshes.

The results obtained make it possible to provide practical recommendations for the design of inclined cross-sections to ensure strength in the areas of local punching of reinforced concrete slabs and shells by an emergency load from an aircraft crash. For such sections, it is necessary to use structural reinforcement in horizontal meshes with a diameter of not more than 16 mm with a step of not more than 100 mm, according (Blikharskyy, 2017; Karkhut, 2021). It is recommended to take the concrete class not lower than C16/20.

Conclusions

1. Under the action of an emergency punching load, the bearing capacity of inclined cross-sections with horizontal reinforcement can be determined according to the design scheme in Fig. 2 according to the refined hypothesis (Eibl, 2003; Makarenko, 1986). In this case, F_n is calculated without the integral reinforcement coefficient, and when calculating F_v, the additional force from the pin effect of reinforcement is taken into account. The tensile strength of concrete R_{bt} is replaced by the value f_{ctm} obtained experimentally when splitting with bars, the diameter of which corresponds to the diameter of the horizontal reinforcement.

2. In monolithic slabs and shells, the installation of additional horizontal reinforcement in the middle of the cross-section height leads to a significant increase in the strength of normal and inclined sections in the zone of punching by an emergency dynamic load; the use of horizontal grids improves the manufacturability of concreting, reliably provides reinforcement anchoring in comparison with vertical stirrups and bends.

3. When calculating the bending moments, the pressure diagram along the length of the external load transfer section should be taken as triangular, in accordance with the provisions of the deformable model adopted in the current standards.

4. To eliminate the risk of fracture from splitting in the plane of the meshes and under the reinforcement bars, it is structurally necessary to use reinforcement with a diameter of not more than 16 mm with a step of not more than 100 mm, according (Blikharskyy, 2017; Karkhut, 2021). It is recommended to take the concrete class not lower than C16/20.

References

Karkhut, I. I. (2015). Temperature loads on reinforced concrete protective structures. - Lviv. Vydavnytstvo Lvivskoi Politehniky (in Ukrainian). https://vlp.com.ua/node/14808.

Eibl, J. (2003). Airplane Impact on Nuclear Power plants. Proceedings of the 17th international conference on structural mechanics in reactor technology (SMiRT 17). Prague, Czech Republic: Vysoka skola technicka. August 17–22. http://inis.iaea.org/search/search.aspx?orig_q=RN:36071655.

Raghupati Roy, U. S. P. Verma and A. S. Warudcar. (1999). Analysis of Massive Reinforced Concrete Ring Beam of Nuclear Containment Structure due to Heat of Hydration. Transactions of the 15th International Conference on Structural Mechanics in Reactor Technology (SMiRT 15). Seoul, Korea, August 15–20. https://repository.lib.ncsu.edu/handle/1840.20/30202.

Briffaut, M., Benboudjema, F., Torrenti, J. M., Hanas, G. (2011). Numerical analysis of the thermal active restrained shrinkage ring test to study the early age behavior of massive concrete structures. *Engineering structures*, 33 (4), 1390–1401. https://doi.org/10.1016/j.engstruct.2010.12.044

Králik Juraj (2014). Safety of Nuclear Power Plants against the Aircraft Attack. *Applied Mechanics and Materials*, Vol 617, 76–80. Online: 2014-08-18©. Trans Tech Publications, Switzerland. DOI: 10.4028/www.scientific.net/AMM.617.76

Makarenko, L. P. (1986). Recommendations for the calculation of reinforced concrete protective shells of nuclear power plants in an emergency, 22 p. Rivne: IIVH (in Russian).

Duan, Z. P., Zhang, L. S., Wen, L. J., Guo, C., Bai, Z. L., Ou, Z. C., Huang, F. L. (2018). Experimental research on impact loading characteristics by full-scale airplane impacting on concrete target. Nucl. Eng. Des., 328, 292–300. DOI: 10.1016/j.nucengdes.2018.01.021.

Luchko, J. J., Mamlin, S. V. (2018). Dynamics of rod systems and structures. Lviv: Kameniar, 524 p. (in Ukrainian). ISBN 978-966-607-416-3. https://www.kamenyar.com.ua/nashi-vydannya/vydannya-2018/160-luchko-j-j-mimlin-s-v-dinamika-sterzhnevikh-sistem-ta-sporud.html.

Sadique, M. R., Iqbal, M. A., Bhargava, P. (2013). Nuclear containment structure subjected to commercial and fighter aircraft crash. Nucl. Eng. Des., 260, 30–46. DOI: 10.1016/j.nucengdes.2013.03.009.

Lo Frano, R., Forasassi, G. (2011). Preliminary evaluation of aircraft impact on a near term nuclear power plant. Nucl. Eng. Des., 241 (12), 5245–5250. DOI: 10.1016/j.nucengdes.2011.11.019.

Babaev, V. M., Bambura, A. M., Pustovoitova, O. M., Reznik, P. A., Stoianov, E. H., Shmukler, V. S. (2015). Practical calculation of elements of reinforced concrete structures by DBN V.2.6-98 compared with the calculations for SNiP 2.03.01–84* I EN 1992-1-1 (Eurocode 2), 208 p. Kharkiv: Zoloti storinky (in Ukrainian). ISBN 978-966-400-327-5.

Karkhut I. I. (2021). Design and construction in areas with high seismic activity. Lviv: Vydavnytstvo Lvivskoi politehniky, 188 p. https://vlp.com.ua/node/20395.

Maksymovych, S., Krochak, O., Karkhut, I., Vashkevych, R. (2021). Experimental Study of Crack Resistance and Shear Strength of Single-Span Reinforced Concrete Beams Under a Concentrated Load at $a/d = 1$. In: Blikharskyy, Z. (eds) Proceedings of EcoComfort 2020. EcoComfort 2020. *Lecture Notes in Civil Engineering*, Vol. 100. Springer, Cham. https://doi.org/10.1007/978-3-030-57340-9_34.

Blikharskyy, Z. Ya., Karkhut, I. I. (2017). Calculation and design of bent reinforced concrete elements, 188 p. Lviv: Vydavnytstvo Lvivskoi politehniky (in Ukrainian). https://vlp.com.ua/node/20235.

Blikharskyy, Z., Khmil, R., Vegera, P. (2017). Shear strength of reinforced concrete beams strengthened by PBO fiber mesh under loading. In: *MATEC Web of Conferences*, Vol. 116, 02006. https://doi.org/10.1051/matecconf/201711602006.

Bobalo, T., Blikharskyy, Y., Vashkevych, R., Volynets M. (2018). Bearing capacity of RC beams reinforced with high strength rebars and steel plate. In: *MATEC Web of conferences*, Vol. 230 02003. https://doi.org/10.1051/matecconf/201823002003.

Selejdak, J., Blikharskyy, Y., Khmil, R., Blikharskyy, Z. (2020). Calculation of Reinforced Concrete Columns Strengthened by CFRP. In: Blikharskyy, Z., Koszelnik, P., Mesaros, P. (eds) Proceedings of CEE 2019. CEE 2019. *Lecture Notes in Civil Engineering*, vol. 47. Springer, Cham. https://doi.org/10.1007/978-3-030-27011-7_51.

Blikharskyy, Y., Khmil, R., Blikharskyy, Z. (2018). Research of RC columns strengthened by carbon FRP under loading. *MATEC Web of conferences* 174, 04017. https://doi.org/10.1051/matecconf/201817404017.

Cavagnis, F., Simões, J.T., Fernández Ruiz, M., Muttoni, A. (2020). Shear strength of members without transverse reinforcements based on development of critical shear crack. *ACI Struct. J.*, 117(1), 103–118. http://dx.doi.org/10.14359/51718012.

Maksymovych S. B., Krochak O. V. (2019). Experimental studies of crack resistance and strength of inclined sections of reinforced concrete beams loaded with concentrated forces. *J. Resour. Saving Mater. Build. Struct.,* 37, 164–174. Rivne: Volynski oberehy (in Ukrainian). ISBN 978-966-416-682-6.

Karkhut, I. (2021). Determining the Stressed-Strained State of Concrete in the Zone of Exposure to Local Laser Radiation. *Eastern-European Journal of Enterprise Technologies,* 3(7(111), 24–36. DOI:10.15587/1729-4061.2021.232671, Available at SSRN: https://ssrn.com/abstract=3887769.

Concrete and reinforced concrete structures made of heavy concrete. Design rules. DSTU B V.2.6-156-2010, National Standard of Ukraine (2011). Kyiv: Ukrarkhbudinform (in Ukrainian).

І. І. Кархут

Національний університет "Львівська політехніка",
кафедра будівельних конструкцій та мостів

МІЦНІСТЬ ПОХИЛИХ ПЕРЕРІЗІВ ЗАЛІЗОБЕТОННИХ ЗАХИСНИХ ОБОЛОНОК ЗА ДІЇ ПРОДАВЛЮВАННЯ

Вивчено досвід армування та підсилення похилих перерізів у зонах впливу поперечних сил та навантаження продавлювання різними матеріалами та конструктивними заходами. Подано результати експериментальних досліджень похилих перерізів захисних конструкцій на ділянці впливу місцевого аварійного навантаження продавлювання. За результатами експериментальних досліджень 12 зразків отримані руйнівні зусилля продавлювання. Наведено результати порівняння розрахунків міцності за різними гіпотезами та методиками для зразків, виготовлених із важкого бетону на портландцементі двох класів міцності на стискання С10/12, С16/20 із застосуванням додаткового горизонтального армування та без нього. В статті наведено армування та міцність похилих перетинів за кута руйнування γ = 40°. Виконано аналіз результатів та розроблено рекомендації із конструювання похилих перерізів тонких плит та оболонок у зоні продавлювання.

Отримані експериментально значення несучої здатності бетонних та залізобетонних зразків під час продавлювання добре корелюють із результатами, теоретично визначеними за залежностями, що враховують нагельний ефект арматури та фактичну міцність бетону. Максимальні відхилення теоретичних значень від експериментальних 0–(+30) % як під час руйнування по похилих, так і по нормальних перетинах. Забезпечити відсутність зминання бетону стержнями та розколювання у площині горизонтальних сіток рекомендовано обмеженням максимальних діаметрів та кроку арматури, мінімального класу бетону. Очевидні технологічні переваги дають змогу рекомендувати застосування на ділянках імовірного прикладання місцевого аварійного динамічного навантаження додаткових горизонтальних сіток замість вертикальних хомутів.

Ключові слова: захисна конструкція; аварія літака; важкий бетон; продавлювання; горизонтальне армування; похилі перерізи.